Global Hyperloop Week 2025

White Paper Submission by

HYPERLINK

Illustration by R. Hasan, Secretary at Hyperlink.

Table of Contents

1. Introduction

1.1 Team Background

Hyperlink is a student-led Hyperloop team based in London. It was founded in September 2020 and is currently operating from Queen Mary, University of London. The team consists of 74 members from Queen Mary, University of London.

Hyperlink was started as the response to meet unfulfilled demand for engineering teams at the Queen Mary, University of London's campus. The team was created to provide ambitious students interested in Hyperloop technology, engineering, and business with dynamic and exciting opportunities to apply their skills in a large-scale project. We are driven by the vision of accelerating the implementation of Hyperloop and developing an innovative mode of transportation.

The team's long-term vision is to create a truly London-wide initiative by uniting the best universities and creating a strong Hyperloop development hub. We believe that London, being one of the world's top technological start-up hubs, would be the perfect place to accelerate the development of the first economically and technologically viable Hyperloop network.

1.2 Development Environment

Our Hyperloop pod is being developed at Queen Mary, University of London campus. For the manufacturing process, Hyperlink is utilising the lab facilities available at the School of Engineering and Materials Science. Moreover, the Engineering department is working closely with Hyperlink's industry partners to gain necessary experience and knowledge. Our industry partners provide the team with assistance on the manufacturing process, verification of the design and its integrity.

1.3 Research Objectives

Hyperloop is a very money and resource consuming project. Skyrocketing costs of technology and infrastructure constitute major limitations and delay towards making Hyperloop a reality. As a team, we want to push the Hyperloop industry forward, making it achievable, inclusive and more sustainable. Therefore, we decided for the theme of the 2024/2025 academic year to be a mixture of **Cost-Effectiveness, Sustainability and Scalability**.

The main research objective is to develop a fully operational pod, reducing production costs by 40%. This is achieved by implementing recycled materials, using a more efficient battery management system and designing a sustainable chassis for the pod.

1.4 Budget

We strive to use our funding effectively to design and build an efficient, sustainable and cost-effective pod aligned with the competition's goals. The approximate budget distribution for Hyperlink is shown in Table 1. The team consistently pursues the objectives of the competition, with our key focus on enhancing cost-effectiveness of the pod system, by strategically planning and incorporating more cost-effective components and exploring the use of recycled materials.

Table 1: Approximate Budget Allocation for Hyperlink

Subsystem	Approximate Amount
Propulsion Subsystem	£2,050
Braking Subsystem	£710
Electronics & Power Subsystem	£280
Test Rig	£1,000
Total System Costs	£3,950

1.5 Hyperlink Representative

The team's representative who will be in correspondence with Hyperloop Global is Jake Oldfield, president of Hyperlink. She can be reached at jakeoldfield2@gmail.com or at +44 7355 645064. If necessary, the team email is: hyperlink@qmsu.org

1.6 Team Members

President: Jake Oldfield
Director of Engineering: Michael Ayres
Director of Research: Charmaine Wong
Project Manager: Tarren Popat
Head of Traction: Shayan Usman
Head of Structures: Jamal Ghazal
Head of Electrical: Ayash Rath
Head of Biomedical Research: Rindhiya Shankar
Head of Scalability: Aryan Kinge
Propulsion Lead: Anuhya Kotakadi
Electronics Lead: Nathaniel Okunwobi
Software Lead: Harry Barnish

Other Members:

Arvyn Khangura	Mahtab Ali	Ashraf Fahim	Om Dutta
Ved Lakhtariya	Carolyn Gwanlam Ng	Jaskiran Kaur Khatkar	Zainab Chohan
Hamna Aziz	Khadijah Zaman	Aaron Mendis	Christo Damai
Omar Elarabi	Ellen Carey	Eniola Fagite	Ashley Phang
Sam Chen Yu	Tsz Wo Bernard Lee	Nizar Tourabi	Ivet Lobo
Nithurshan Manoranjan	Erik Croitoru	Brandon Rutagamirwa	Rohit Singh
Zafirah Bhatti	Tanisha Srivastava	Dheekshitha Sendil	Mustafa Sahin
Kwaku Dwamena	Ogulcan Gurelli	Ali Salaheldin	Yaz Yagmur Sahin
Abdirahman Farah	Shamia Akhter	Enea Caushi	Jackson Chidiac
Hiresh Rughwani	Hashem Bahamedan	Samantha Dias	Michaela Shakespeare
Morshid Sarker	Dhyey Ketan Joshi	Maneeha Siddiki	Mohammed Miah
Bilal Qureshi	Shray Thakker	Muhammad Khan	Mohammed Hegy
Berfin Kaya	Rawan Ahmed	Natalia-Diana Miron	Kevin Mateos
Wing Yu Tse	Vismika Jeyabalan	Supraja Jayakumar	Navya Narula
Lea Edwards	Rukevwe Marissa Udi	Emile Abrantes	Sheena Varghese

2. System

2.1 Technical Description

The Hyperlink's innovative transportation pod is intricately designed with a paramount focus on high-speed propulsion, safety, adaptability, and cost-effectiveness. The system comprises of six key subsystems: propulsion, braking, structures, suspension, and electronics, including power, with software. This design adheres to strict constraints, with a maximum weight of 100 kg and approximate dimensions specified as 1.65 m by 0.52 m by 0.3 m (length x width x height). The overarching goal is to balance high-speed performance, safety, adaptability, and cost-effectiveness.

To achieve high-speed performance, the Hyperlink pod relies on a Dual Linear Induction Motor (DLIM), with each powered Linear Induction Motor (LIM) on each side of the pod, designed for scalability and cost-effectiveness, with a target top speed of 30 km/h. The designed LIM features a laminated silicon steel stator wound with rectangular copper coils, to improve speed and efficiency, and a moving aluminium rotor attached to the pod frame. The propulsion team focuses on the stator sheet thickness, wire cross-sections, winding configurations, and a multi-phase linear induction motor. The multi-phase inverter design is also explored, to allow better efficiency across speeds. One aspect of ongoing research is on electrical configurations, to optimise magnetic flux generation while minimizing power losses. The goal is to achieve a practical, high-speed propulsion system to meet our overarching goal. Further information on Propulsion's subsystem is found in 2.2 Propulsion.

Commented [OC1]: Inconsistent top speed, please adhere to a single speed.

The braking system integrates primary eddy current brakes and secondary friction brakes for efficient deceleration and safety. The safety considerations encompass both fail-safe emergency braking and thermal management. With both eddy brakes using neodymium Halbach arrays, which induce currents in an I-beam to generate braking force, and friction brakes, which employ carbon ceramic pads, ensures controlled braking and functionality even during power failure. Both types of brakes are engaged via spring systems that are held in compression by electromagnets and are released when braking is activated. A designed test-rig will be used to simulate the braking system's performance. The integrated braking system aims to balance efficient deceleration with safety through deliberate design choices and ongoing improvements. Further information on Braking's subsystem is found in 2.3 Braking.

The electronics system, with its designed software, is responsible for the pod's power delivery, control and communication operations. The electronics system is divided into two different subsystems in terms of power delivery – the "High Voltage System (HVS)", which operates at 48V for the propulsion, and the "Low Voltage System (LVS)", which operates at 24V, which is responsible for the rest of the systems. The power is delivered from lithium polymer batteries integrated with a Battery Management System (BMS). Testing for the system involves verification of the sensors, communication tasks, power supply and the system's integration with the propulsion and braking systems. The team responsible for the circuit aims to work towards improving the system's overall stability, exploring the design of master-slave architecture based embedded systems to introduce modularity, improving the structural stability and improving the system's interfaces. The software subsystem comprises the onboard communication layer for the embedded systems, software for remote control and telemetry of the system, and an interface to control the system and view and visualise the telemetry data. The software system aims to facilitate safe and stable pod operations.

Further information on Electronics and Software subsystems is found in 2.4 Electronics – Power, Control, Communication & Software.

The safety section, identified as Section 3.Safety, details the safety for each of the systems in Table 8Table 9Table 10. The section covers various aspects such as the current overload, short circuit, magnetic field impacts, overheating and structural stability, among others, to ensure the measures taken are comprehensive and cover a range of potential issues.

In conclusion, the Hyperlink pod system is a multidisciplinary design endeavour, aiming to achieve a balance between high-speed performance, safety, adaptability, and cost-effectiveness. The constraints and values outlined in the tables below guide the development process, ensuring the system meets the specified criteria. The forthcoming sections will delve deeper into specific aspects of each subsystem, providing a comprehensive understanding of the design choices and their implications.

Table 2: System Constraints

System		Demonstration	
Length	>1650 mm	Levitation Height	-
Width	>520 mm	Maximum Speed	30 km/h
Height	>300 mm	Maximum Acceleration	1.377 m/s^2
Weight	<100 kg	Maximum Deceleration	6.940 m/s^2

Commented [OC2]: Very ambitious. I would suggest 20 km/h

Table 3: Traction System Characteristics

(Propulsion and Braking Subsystems)

Traction System	
Maximum Acceleration	1.377 m/s^2
Maximum Deceleration	6.940 m/s^2
Operating Voltage	48V
Nominal Current	25-30A
Maximum Power	1440W
Dimensions	- For stator sheet: 500x100x50mm - For Halbach array: 500x40x10.5mm
Braking distance @ V_{max}	30m (25m for Eddy braking and 5m for Friction brakes)

Commented [OC3]: Peak current would be nice to mention if possible.

Table 4: Electrical System Characteristics

Electrical System			
HV Battery (x 2)		LV Battery	
(Battery Type	Lithium Polymer	Battery Type	Lithium Polymer
Capacity	5000mAh	Capacity	2700mAh
Nominal Voltage	22.2V	Nominal Voltage	22.2V
Cell configuration	6S	Cell configuration	6S
Max. Discharge current	750A	Max. Discharge current	175.5 A
Weight	840 g	Weight	401 g
Dimensions	170 x 48 x 53 mm	Dimensions	133 x 42 x 31 mm
Software Subsystem			
Board Communication Protocols		CAN, TCP/IP	

2.2 Propulsion

The propulsion design for this year prioritises scalability and cost effectiveness, with a targeted speed of 30 km/h. This means creating a system that can be efficiently adapted to different scales while maintaining economic feasibility. This approach ensures application flexibility and resource efficiency, in line with the overarching goal of achieving optimal performance within practical constraints.

The propulsion system will be a linear induction motor (LIM) which comprises of two components: a stator and rotor. Between October 18th and December 5th 2024, the stator core design unfolded in three key phases: extensive research, application of research findings for upgrades to last year's design, and CAD drawing creation for the new windings. The stator will be the design focus and is a core made of welded steel sheets with copper wire windings (Ion Boldea, 2017). During this initial design document, four key aspects will be discussed, three of which will be implemented in our final design review: stator sheet thickness, wire cross-sectional dimensions, compact winding configurations, and the implementation of a 6-phase inverter to the design.

Prototypes with different winding configurations will be constructed for testing at Queen Mary, University of London's lab facilities. The propulsion system will undergo testing at full-speed and power trials, to evaluate the LIM's highest speed, thrust force, and energy losses. Safety parameters, including thermal and electrical considerations, are integrated into the design to prevent overheating and ensure reliable operation.

The safety considerations will focus around thermal and electrical safety. Thermal safety is addressed through applying techniques like air cooling and cold plates, along with continuous temperature monitoring during testing. Electrical safety is a priority due to the high-voltage three-phase electrical supply. Insulation measures, such as using electrical grade resin, are implemented. Emergency protocols are in place, triggering brakes and halting the pod in case of any component failure.

The stator design involves considerations such as size, material selection, winding configuration, and wire design, which must be designed in a way to achieve better performance through increased thrust. Understanding the functions and effects of each design element proved to be a challenging task of this process but with the guidance of mentors and extensive research done online, the team developed an

Commented [SU4]: As the old system went up to 50km/h (31mph) I want the target speed to be around 50mph (**81km/h**)

Commented [MOU5]: This needs updating

Commented [SU6]: As you have mentioned 'Four Key Aspects, You've only listed 3. We know what they are but they don't.

Commented [SU7]: No need to change, this stays the same.

Commented [SU8]: three-phase is correct

Commented [SU9]: This is correct, no need to change

Commented [SU10]: Reword this with something like: The new stator design involves consideration like size, material selection, and better performance along with its efficiency.

Commented [SU11R10]: The 'and better performance along with its efficiency' part try to reword that part to make it sound better than what I said.

understanding that allowed for effective design choices. Subsequently, the team faced another difficult challenge, prioritizing which design elements to prioritize for the improvement of the motor efficiency. The outcomes of this analysis will be examined in greater detail in the following subsections.

2.2.1 Stator Sheet

The stator being manufactured for this year's demonstrations will be made from sheets of non – orientated silicon steel (72251900) with thickness of 0.1mm-0.5mm. Silicon steel is an alloy of iron with silicon which improves its electrical efficiency and magnetic properties. Specifically, non-orientated silicon steel was chosen due to its isotropic magnetic properties of varying flux in all directions unlike oriented silicon steel, which has a preferred direction of magnetization. Non-orientated silicon steel is also a soft magnet which allows for rapid changes in magnetic field, hence enhancing the magnetic flux that will be produced by the coils by minimising energy loss through raising electrical resistivity (Chiba, A. 2005). Additionally, silicon steel has high permeability meaning the material can align to the magnetic field easily, resulting in less eddy losses and less hysteresis's losses due to low coercivity which will improve the efficiency of the LIM. Lastly, in silicon steel, temperature has a small effect on the magnetic properties which is crucial for longevity and performance (Shcherbakov, P. 2004).

Commented [DB12]: say that its non-oriented and expalin the benefits of using non oriented compared to oriented. Also, silicon steel but mention its manufacture code, which excatly type are we using. Us the material that I have sent to at least propose thickness optimization

The dimensions for the stator sheet will be 500mm x 100mm x 0.1-0.5mm. Thin sheets reduce the surface area that eddy currents travel through, thus, reducing losses via eddy currents. Also, thin sheets improve heat dissipation which is important as it will reduce the overheating of the LIM (Electrification, C. 2021). Any additional benefits and optimisation of this design choice will be explored further in the PDR.

2.2.2 Wire Cross-Sectional Analysis

Table 5: Key parameters discussing the differences in wire cross-section in comparison to previous model.

Parameters	Effects on efficiency
Fill Factor	Enhanced wire packing, compared to circular wires, improves fill factor by efficiently occupying the same space, increasing current capacity, power density and motor output. The refined packing, alloy composition, and varnish application collectively enhance a wiring system's performance, offering increased power capacity and stability. Different wire winding arrangements simplify motor construction, reducing insulation damage and short circuits, ultimately optimising overall performance and operational safety. [WMD-sonja, 2022]
Space efficiency and weight reduction	The flat profile of the rectangular wire's advantages in efficient stacking and arrangement in tight spaces and where stator slots are closely spaced. The malleability of rectangular wires [Copper Development Association, Nd] enables a denser packing compared to round wires, leading to enhanced efficiency for (LIM) by reducing energy losses and improving overall performance. Furthermore, rectangular wires results in a reduction of material usage compared to a similar round wire conductivity. The equivalent cross-sectional area of rectangular wires in comparison to the round wires reduces the overall size, leading to weight reduction.
Reduced Skin effect	The reduced skin effect allows greater distribution of current uniformly by allowing greater frequency to be applied [Skin effect, 2023], the higher the uniformness, the lower resistance experienced which therefore allows

Parameters	Effects on efficiency
	greater power output. This will enable more uniform current to flow closer to the core of the LIM and allow a more efficient use of higher frequencies and as a result more power is generated. [Electrical4U, 2023]
Enhanced Cooling	Rectangular wires have a larger surface area compared to round wires which results in contact with the surrounding environment which allows greater heat dissipation to the surrounding environment. The larger surface area also allows for convection and radiation heat transfers as the wire heats up (the increased surface area allows more efficient exchange of heat). [The physics classroom tutorial ,2023] In minimising heat build-up and reducing the risk of overheating, rectangular wire contributes to the aspects of the electronic components. [Ningbo Jintian Copper Group Co., Ltd., 2023]

The short-term goal of this aspect is to verify whether the rectangular wires outperform the circular ones in the COMSOL simulation. The final goal would be to apply the optimal design into the final demonstration.

2.2.3 Winding Configurations

Another key design element for the linear induction motor is the winding of the wires which has two effects on the motor's performance: acceleration and velocity. In accordance with this year's theme of cost effectiveness, the focus will be on reducing the cost while simultaneously improving the motor's acceleration. This will be especially impactful when the pod begins to be scaled up and cost efficiency will be important for accelerating a pod of greater mass. For the demonstration, two winding configurations will be explored through simulation to determine which will be more successful with the pod. One will be a standard 3 phase overlapping configuration as portrayed in *Figure 2.2.3.1* and the other configuration will be an adjacent winding configuration as in *Figure 2.2.3.2* (Ion Boldea, 2017, p59). The design that shows the most successful will be constructed and undergo the testing mentioned above.

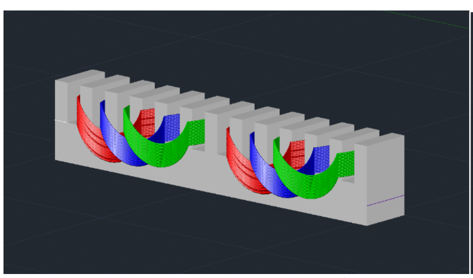

Figure 2.2.3.1: 3-Phase Overlapping Wire Configuration.

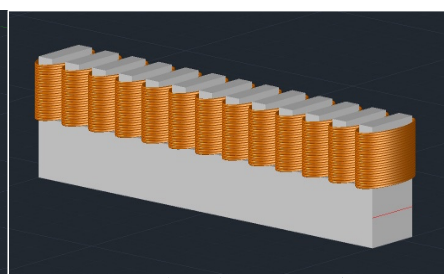

Figure 2.2.3.2: 3-Phase Adjacent Wire Configuration

2.2.4 Multiphase Linear Induction Motor

The last element of the LIM that will be included in the demonstration document as in-depth investigation will be the implementation of a multiphase linear induction motor design; a system that would utilise both a 3-phase and 6-phase system. The intention of this design would be to have the 3-phase system be able to switch to the higher phases after acceleration past lower velocities. This would provide the benefit of

Commented [DB13]: can you please make references, this is very good but i need to know why and if i can trust this. Definitely good content though

Commented [JS14]: @Shayan Usman this is mentioned in both @Jarifa Tasnim Shah and @Yaminur Rahman paragraphs under space efficiency and enhanced cooling method- should we only stick to one instead of both?

Commented [SU15R14]: mention both as it links with each other

Commented [SU16]: might change to 'cost effectiveness' as a theme achieving greater terminal velocity through the 6-phase system without losing the greater 3-phase acceleration during the initial acceleration. Unfortunately, due to budget restraints, this element of the motor's design will stay theoretical but will be explored through COMSOL simulations and theory.

There are 2 main elements which determine the velocity that the motor can achieve: the winding of the wires and the speed at which the magnetic field travels across the surface of the secondary stator. This element focuses on changing the speed which the magnetic field travels across the stator. Typically, to increase this, the three-phase inverter is exposed to an AC current at a higher frequency which results the in the electromagnets changing their polarity at an increased rate. The idea behind the 6-phase inverter is to increase the wavelength of the variation across the inverter while maintaining the frequency. Under these changes, the wave equation shows that the speed of the wave would increase, thus the velocity of the magnetic flux would increase as well. However, compared to the 3-phase inverter, the 6-phase inverter would be less efficient at lower velocities due to there being less magnetic flux over the same distance. This problem created the idea for a multiphase design where the motor can be switched from a 3-phase system to a 6-phase system as it reaches higher velocities. This design would perform similarly to a gearbox so that it may perform more efficiently at varying velocities.

Commented [SU17]: instead of saying this, mention the use of a gearbox because of this.

2.2.5 Challenges, Further Work and PDR

The evolution of the design involves addressing cost challenges associated with scaling up the LIM for high power applications, impacting components such as stator sheets and wire configurations. Variations in stator blade thickness were found in research to directly affect power conversion efficiency by reducing electrical losses when changing energy into magnetic flux. Additionally, to maintain efficiency and prevent heat build-up, optimising wire configurations by ensuring precise and uniform winding of the wire coils by avoiding inconsistencies in magnetic fields or potential short circuits, which can lead to electrical faults.

Budgetary constraints have significantly influenced decisions regarding material selection and production techniques. Future work and PDR will be focusing on specifying propulsion power requirements, mounting fixtures, finite element analysis results, test rig construction, experiment results, and safety protocols. Additionally, computational simulations utilising COMSOL will be employed to model operational principles, assess side effects, and pinpoint potential failure points. This comprehensive approach in the design aims to optimize the system to its maximum potential.

2.3 Braking

2.3.1 Description of Braking

The braking system will consist of a primary eddy current and secondary friction brakes that utilises a brake pad. The friction brakes will have a dual purpose as emergency brakes in the event of braking failure.

The initial design process started with developing and understanding of the key components and physics of the eddy current braking system. Friction brake types and materials were researched and reviewed on how it would affect the braking dynamics/physics and affect the overall structure of the pod. Budget constraints also influenced the decision. This knowledge, of both eddy current and friction brakes, helped set the foundation of the design criteria and targets. The design was made using a combination of in-depth research conducted on eddy currents from online sources and from last year's findings, to create an effective braking system to stop the pod.

The eddy-braking system features two magnetic couples fashioned in a "C" shaped manner, using two neodymium Halbach arrays. These couples are fixed to sliding guide rails on either side, which are moved towards the I-beam via a spring system held in compression by electromagnets, which is represented in Figure 2.3.2.2. Neodymium magnets are composed of microcrystalline grains which allow the magnets to have a high magnetic strength whilst maintaining durability and efficiency (Nogah, C, 2023). The magnetic flux induces eddy currents within the I-beam, which exerts a force against the magnets, inducing a braking effect according to Lenz's law, derived from Faraday's law (Boldea, I., 2023):

Commented [DB18]: Give the references from the book I will send you

$$\varepsilon = \frac{d\phi_B}{dt}$$

Where ε is the induced electromotive force and ϕ_B is the magnetic flux.

$$\phi_B = BA\cos\theta$$

Where B is the magnetic field strength, A surface area and θ is the angle of the field lines to the normal of the plane. The braking force of the magnetic array will depend proportionally on the strength of the permanent neodymium magnets, and inversely proportional to the distance from the array to the I-beam, which will maximise B. A longer array will maximise area, A, but this will force a trade-off between brake force and mass.

The friction braking system consists of a carbon ceramic brake pad being used to halt the pod, which will be lowered onto the top of the I-beam to decelerate the pod after eddy current braking occurs. The system utilises a similar spring system to that of the eddy current system, featuring a spring system held back in compression using an electromagnet. When the electromagnet is disengaged, the brake pad is propelled towards the I-beam, and braking occurs once the pad and the I-beam encounter one another.

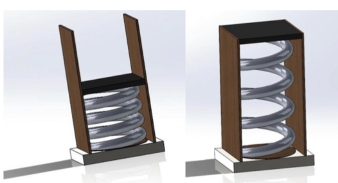

Figure 2.3.1.1: Friction Brakes when Disengaged and Engaged

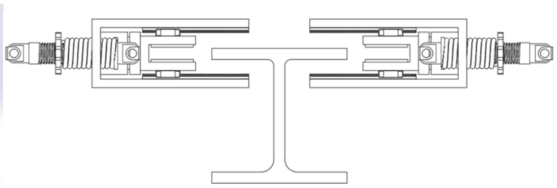

Figure 2.3.1.2: Eddy current brakes schematic spring system.

2.3.2 Permanent Arrangement of Magnets (Halbach Array)

A Halbach array is an array of permanent magnets that have cyclic, shifted orientations of individual magnets that augment the magnetic field strength on one side of the array while reducing the field strength of the other side to a minimal level. Increased amounts of arrays used in the design, maximises the available surface area interaction between the magnets and the conductive rail, producing a greater force at a given velocity, as visualised in the following diagram.

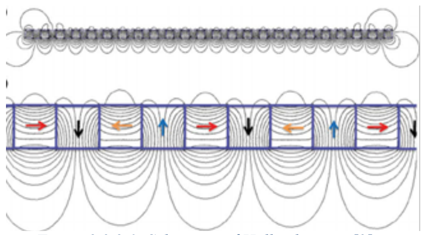

Figure 2.3.2.1: Schematic of Halbach array [3]

Figure 2.3.2.2 illustrates the operational sequence of the braking system during pod travel. The plates, the magnets are mounted on, will withdraw from the I-beam while the pod is in motion, causing the eddy current braking mechanism to be disengaged for unrestricted acceleration. After the pod reaches a set RPM (equivalent to the top speed), the LIM motor will shut down and the eddy brake springs will move the array horizontally towards the I-beam, inducing eddy currents within the I-beam that will decelerate the pod to a low speed, but not to a halt. The linear friction brakes will then engage via the spring system and bring the pod to a complete halt.

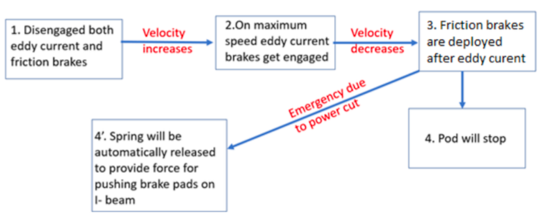

Figure 2.3.2.2: Simple Flow Diagram of the Braking System

2.3.3 Size, Components & Appearance

1. **Magnetic Couple** consists of two neodymium Halbach arrays that amplifies the magnetic field in one direction towards the I-beam.
2. **The inner C channel** holds the permanent magnets in the desired magnetic couple configuration.
3. **Linear rails** are guide rails that are designed to allow for smooth and precise linear motion of the inner C channel that houses the magnetic couples. These consists of a track and a carriage that moves along the track, providing support and guidance for the component.
4. **Outer C channel** provides the following purposes:
    a) Assists in connecting the eddy current braking system to overall structure.
    b) Protects linear rails and inner C channel from external damage, i.e. impacts or vibrations.
    c) Provides support for the linear rails and the inner C channel.
    d) Prevents leakages in magnetic field flux that may be produced by the system, reducing the potential for interference with other components.
5. **Electromagnet and magnet**- 12 V DC electromagnet and magnet holds both eddy current and the frictional braking systems in its disengaged state until the pod brakes. The default state of the system is disengaged as the electromagnets hold back both systems. When the electromagnet loses power, the brakes are automatically engaged.

6. **Coil Springs** are responsible for changing the state of the mechanical and eddy current system from engaged to disengaged by transferring stored elastic potential energy into kinetic energy of the linear rails.
7. **Pads** will be utilised for the frictional brakes made of carbon ceramic, which has a high material resistance to wear and damage tolerance for frictional braking on the I-beam.

2.3.4 Eddy Current Test Rig

The test rig is used to simulate the braking system's theory to be used on the actual pod, with a rotating aluminium disc, powered by the LIM motor, replicating the pod's interaction with the I-beam. The test rig's braking system features one magnetic couple consisting of 2 C-shaped Halbach arrays, positioned near the disc edge and is held back via a spring, held in compression by an electromagnet. Once the electromagnet is deactivated, the spring will propel the magnetic couple towards the rotating disc, causing the disc to brake using eddy currents. The following is a list of the components to be used:

- 2 magnetic arrays creating a magnetic couple made from N42 neodymium magnets.
- An aluminium disc with a thickness of 10 mm and a diameter of 800 mm.
- A test bench which holds the whole system together.
- Sliders to slide the couple forward and back from the aluminium disc.
- Springs to hold the couple away from the disc.
- An electromagnet to hold the spring in a compressed form.

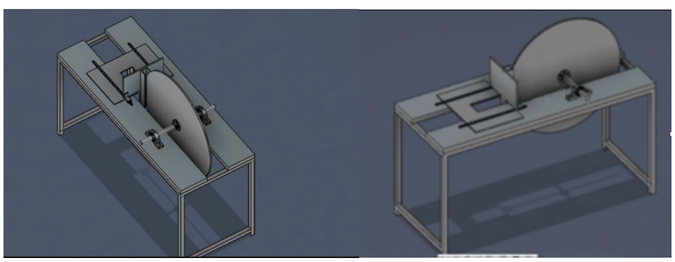

Figure 2.3.4.1: Drawing of the Test Rig Build

2.3.5 Constraints

Commented [BKD19]: Do we need this here or is this in section 4

Table 6: Braking System's Constraints

Constraints	Details
Spring System for Eddy Current Brakes	• The system is spring loaded where coil springs are used to hold back the array from the I-beam; these will be held in compression via electromagnets and will spring forward once the electromagnets are released, allowing braking to occur. These springs will have to be manually recompressed due to the spring-loaded nature of our system.

Constraints	Details
Spring System for Friction Brakes	• The mechanical friction brakes are spring loaded, they utilise coil springs to hold the system in compression. The system features the same electromagnetic spring-loaded system used in the eddy current braking system. This therefore means it will also have to be manually compressed.

Further details on specific safety features will be covered in Section 4. Appendices

Commented [TP20R19]: stays here i think

Details of the Design Process

Before choosing eddy current braking as our primary braking method, a range of other different braking methods were explored, such as hydraulic and pneumatic braking methods. However, due to eddy current braking being highly effective at high speeds and causing little to no wear on the components, this was chosen as our primary braking system. The eddy current braking is less effective at low speeds since the braking force is directly proportionate to the speed of the pod. To stop the pod at low speeds, a friction braking system was introduced to work in unison with the eddy current brakes. The design for the friction brakes was relatively simple as the pod will only use this at very low speeds: the pad used will be a carbon ceramic as it allows a good amount of braking force applied, without harming the I-beam.

Moving from conceptualisation to tangible models, sketches of the brake components were generated into CAD models. The team also conducted FMEA to identify the potential failures, know their causes and effects, and what could be done to build a better system. As we progress, COMSOL simulations and analysis will be done to complete the initial concept and design stage and move onto manufacturing and testing phase.

2.3.6 Challenges and Further Improvements

One of the main challenges was knowing where the friction brake system needed to be placed within the chassis, due to the limited space. Depending on where the system was going to be applied either on the I-beam or physical rotating disk, required extensive communication with other team heads to ensure the braking system would seamlessly integrate with the structure and other subsystems, without causing interference with their respective hardware components.

In our earlier description about the build of the test rig, we mentioned the use of two arrays. Currently, the team possesses one array, however, our aim to incorporate an additional array to complete the test rig. This will allow the team to create the magnetic couple mentioned in section 2.3.4 Eddy Current Test Rig, which is essential for the braking's system effective operation. Alongside increasing the number of arrays, COMSOL simulations and analysis will be done to finalise the initial concept and design and move onto manufacturing and testing phase.

2.4 Electronics – Power, Control, Communication & Software

2.4.1 Description of Electronics – Power, Control & Communication

The electrical subsystem is divided into "High Voltage System (HVS)" and "Low Voltage System (LVS)" and are powered by 44.4V and 22.2V lithium-polymer batteries respectively. It ensures reliable, safe power supply and continuous monitoring of the pod status via a Controller Area Network (CAN) bus integrated with the On-board computer (OBC). The HVS delivers power to the propulsion system through the inverter to the linear induction motors (LIM), while the LVS handles powering the inverter for the LIM, managing the braking sub-system, and the voltage of LVS is stepped down to 5V to provide power to the rest of the components. The 3-phase Unitek Bamobil D3 inverter was chosen because of its power output of 3.8 kW, its easy-to-use configuration software and support for CAN bus communication.

Power – Figure 4.1.1 in Appendices

- **Dual Voltage System:** The electrical subsystem consists of two smaller subsystems, and the low voltage system has a redundancy of one (responsible for controlling the braking system), thus improving reliability.
- **Propulsion Power Delivery:** The HVS powers the propulsion system, directing energy through a DC/AC inverter (Figure 4.1.4) to the linear induction motors (LIMs).
- **Battery Management Systems (BMS):** Specific BMS modules are being explored, where the BD-AP21S001 BMS has emerged as the leading choice for HVS. It is essential for monitoring and protecting battery packs and managing charging states, voltage, current, and cell temperature. It supports rapid charging and discharging for enhanced efficiency. BMS is implemented in a distributed battery topology to protect the battery packs and monitor the charging state, pack voltage and current, and cell temperature.
- **Battery Specifications:** A 12S 44.4V lithium-polymer battery is used for the HVS and a 6S 22.2V lithium-polymer battery for the LVS. Thus, these batteries allow us to not only support a voltage rating close enough to the targets of 48V and 24V but also have high C ratings, therefore capable of supplying the required current for the propulsion and breaking sub-systems.

Please see the safety aspects for Power explained in Table 10 in Section “3.Safety”.

Control – Figure 4.1.2 in Appendices

- **Inverter Selection:** A 3-phase Unitek Bamobil D3 inverter is employed for its 3.8 kW power output and CAN bus compatibility. It converts from DC to AC to power the LIM. The inverter comes with its configuration software called “Ndrive,” which allows control of the acceleration and deceleration of the LIM. The software dashboard displays other metrics, including velocity, temperature, and power.
- **Sensor Board Functionality:** It monitors vital variables like velocity, acceleration, position, and orientation using Inertial Measurement Unit and encoders. Temperature sensors in the propulsion system oversee the LIMs' temperature.
- **Relay-Managed Braking:** An 8-channel relay board, is used for the pod's braking operations. These relays are controlled by the board, allowing for the precise engagement or disengagement of the braking system in response to various operational conditions.
- **Control Panel:** Various LED indicators are installed on the control panel to provide visual signifiers about the system's current state. The e-stop (emergency stop) is also mounted on the control panel, giving easy access to cut the HV power without unplugging components.
- **Other features:** The remote override switch is connected to the OBC to remotely turn on the system and disengage the brakes if the braking board fails.

Please see the safety aspects for Control explained in Table 10 in Section “3.Safety”.

Communication

- The OBC controls power and electronic devices through the CAN bus network using a USB to CAN bus transceiver. Some modules and switches are managed remotely via WiFi. The OBC also interfaces between the vehicle and the control station for uninterrupted commands and data exchange.

- The OBC will communicate with the UI using ICP/IP.
- The inverter uses the CAN bus network to allow for bi-directional communication. The inverter can send information about its status and receive commands from ROS over the CAN bus network. The SocketCAN interface enables interaction between the ROS node to send and receive CAN messages containing the inverter's data metrics.
- The BMSes for both LV and HV batteries have CAN bus interface to send messages about the battery packs' metrics to display on the GUI.
- The braking board and sensor board communicate through CAN bus protocol.

Please see the safety aspects for Communication explained in Table 10 in Section "3.Safety".

Testing Plan Prior to Competition

<u>Relays:</u>

1. Check both the communication within the system and the remote communication from "Mission Control" and the electronical system.
2. Test each relay individually by the OBC.
3. Control Each relay manually using a software program to switch them on and off.

<u>Inverter:</u>

1. Check if the inverter is responding through its software.
2. Ensure communication from inverter to the OBC.
3. Test proper power supply to the LIMs for a specific period.
4. Accelerate and decelerate the pod through commands from the OBC.

<u>BMS:</u>

1. Log data of the battery state and display on the GUI.
2. Charge and discharge batteries while wiring up to the BMS.
3. Integrate with the rest of electrical subsystem to guarantee seamless power supply.

<u>Sensor Board:</u>

1. Flash testing programs into the sensor board to verify communication to the OBC.
2. Connect it with other subsystem each at a time and check for proper data acquisition.
3. Integrate it with brakes and motors and make decisions according to input data.

Research and Decision-Making Process

Throughout the design process, the Electronics Team utilized a combination of theoretical research, practical component testing, and iterative development. Research involved analysing data sheets, understanding physical communication protocols, and evaluating the thermal behaviour of the system components under various operating conditions. Testing included ensuring seamless communication and verifying the proper operation of the Battery Management Systems (BMS) and relay boards.

The team's approach to design was grounded in collaborative brainstorming, leveraging the diverse expertise within the group to innovate solutions that met both the technical and safety criteria. The research done was aimed at selecting components that would offer the best integration into the Hyperloop system while providing the necessary robustness and reliability for the pod's operation.

2.4.2 Challenges and Further Work for Electronics – Power, Control & Communication

The team is currently working on the overheat protection, particularly, for the inverter as a major controlling unit, as we used to confront errors about overheating components. Currently, the sensor board and the braking board have been integrated into one telemetry PCB. To circumvent, the telemetry board is used only as a sensor board while the brakes are handled by a manufactured relay board. For future improvements, more sensors will be implemented with the sensor board for accurate tracking of the system. A pressure management system with sensors and actuators is planned for vacuum operation monitoring. The current 3-phase inverter will be replaced by a 6-phase inverter to improve propulsion.

2.4.3 Components List

Table 7: Electrical System Components List

Category	Components & Characteristics
Batteries and BMS	LiPo Battery (44.4VDC) 2 LiPo Battery (22.2VDC) JBD Smart 8-21S BMS (48V, 150A) Li-ion BMS PCB Daly (24V, 20A) Battery Charger (6S-12S) Battery Selector Circuit
Safety Switches and Relays	8-Channel Relay card with CAN interface 48V-battery disconnect relay Insulation Monitoring Relay Remote override switch Negative and positive pole relay 3-pole motor relay E-stop
Sensor Board	Inertial Measurement Unit Temperature Sensors Pressure Sensors Accelerometers Noise Sensors (Rotary Encoder) Inertial Measurement Unit
Other Modules	Wifi Module Jetson Nano Induction Motor Driver - Unitek Bamocar D3 ESP32

2.4.4 Description of Software and System Architecture

The software facilitates the transmission of data between the components of the system and provides a centralized process for monitoring, controlling, and visualizing the subsystems to ensure a safe and cohesive system. The architecture of the system outlined in Appendix Figure 4.1.7 consists of a CAN bus networking layer for the electrical components, a finite state machine (FSM), middleware service for ingesting and transforming data from the electrical components, and a graphical user interface (GUI) for visualizing and interacting with the subsystems. The architecture for the software components was designed at the end of the previous academic year, so the focus of this year is to implement a strong foundation for the design below with frameworks that are easy to integrate and share a common programming language.

2.4.4.1 Network & Communication

The Control Area Network (CAN) bus is the primary communication protocol used between electrical boards, and the socketCAN open-source drivers allow communication between the CAN-bus embedded system board and Linux-based network. For electronics, this means access to the board's inputs and outputs at varying bit rates to access sensor data to deliver instructions to the different boards. The socketCAN library provides APIs to allow the computer to communicate with devices through a common interface. The data from the devices will be transmitted to the ROS middleware service through TCP/IP and then to a remote computer that contains the GUI.

2.4.4.2 Finite State Machine (FSM)

The on-board computer (OBC) runs an Ubuntu-based GNU/Linux distribution called Jetpack provided by Nvidia. The OBC will host the FSM that manages the safety and stability of the pod by processing the CAN bus packets from the electrical components and ROS messages from the GUI. The FSM will use this data to manage the relevant states outlined below:

- **Idle** - Pod powered on and all subsystems online, brakes engaged by default and propulsion system not active.
- **Setup** - Once all safety checks, connectivity checks, and sensor calibration shave taken place successfully.
- **Acceleration** - After the launch signal is triggered, the brakes are disengaged, the propulsion system is activated, and the pod begins to accelerate reaching a peak speed of 150km/h and this state is where the most safety risk arises.
- **Cruise** - Upon reaching cruising distance, the pod stops accelerating and continues its trajectory, the thrust is reduced to match the force of the linear Halbach array to maintain a constant speed.
- **Deceleration** - After cruise distance is covered or the minimum braking distance is approached, the propulsion is switched off and the pod begins normal deceleration, engaging the brakes.
- **Safe Abort** - If any errors occur or internal or external connectivity is lost then the pod's trajectory is stopped by engaging the primary brakes and cutting power to the propulsion subsystem.
- **Power down** -When the pod has reached a standstill and the brakes are engaged, the pod will power down and will emit the powered down signal.

2.4.4.3 Graphical User Interface (GUI)

A Graphical User Interface (GUI) will serve as a centralized liaison between the engineers and the subsystems of the pod. The GUI, as shown in Appendix Figure 4.1.8, is integrated with the ROS middleware service to visualize various important data of the system, such as temperature and power. It also provides a debugging console to inform the engineers of any issues, and various control options such as buttons for switching on/off the system and applying the brakes. Solara is the framework used to develop the GUI since it reduces the programming requirements for developers and allows for faster workflows.

An objective for this year is to also integrate simulated data from COMSOL that represents the behaviors of the subsystems to improve the testing of new software features and decouple the dependencies on physical installations of the electrical components. Enabling this parallel workstream will greatly improve the velocity of developing and testing new software features.

2.4.4.5 Challenges and Future Work for Software

The biggest challenges this year involve the integration of CAN bus with the physical electrical components and transmitting the related data to the GUI through TCP/IP which are mostly a result of the lack of familiarity implementing these components. Below is a list of some of the future work for the software team:

- Integrate CAN bus with the inverter and BSM electrical components.
- Between the FSM and the GUI.
- Integrate the GUI with simulation tools like COMSOL to test new features and observe system behaviors.

3.Safety

Table 8: Propulsion System's Safety Features

Safety	Details
Current Overload	Software systems will maintain the current input below the maximum current load of the wires.
Short Circuit	Check that all terminals are screwed down and connections are secured. Check system has continuity between start and terminals. Check the insulation rating between windings and stator.
Magnetic Field Damages Other Components	This will be tested once the pod is complete. If still problematic a shield will be made. Simulations indicate the field is equivalent to 0-100mm from LIM.
Linear Induction Motor Overheating	Have thermal sensors that disable the propulsion system if temperature is too great.

Table 9: Braking System's Safety Features

Safety	Details
Brake Structure	• Requires structural integrity of subcomponents to withstand such forces to avoid catastrophic failure.
Mechanical Friction Brake Actuators	• Springs must always be held back, loaded in its engaged state. Accidental trigger of the springs during motion could cause excessive wear of the friction brakes whilst propulsion systems are still active. Could cause potential damage to the mechanical components of the pod.
Emergency Brakes	• The brake pads must automatically engage on the I-beam to halt the pod in the event of an incident, electrical/mechanical failure. Both braking systems will brake when pod loses power.
Thermal Safety	• Over-reliance on friction brake can produce heat resulting in material failure and damage to electrical & mechanical components. Must be used only to bring pod to a complete stop or exist as the main system for the emergency braking of the pod as a fail-safe mechanism.
Dimensions and Placement	• Placement of the mechanical braking system consisting of the brake pads must be placed leaving sufficient space for remaining assembly of the pod whilst ensuring structural stability.

Table 10: Electrical System's Safety Features

Power	
Safety Structure	**Details**
Power Supply	Both high voltage and low voltage batteries are wired to a BMS to monitor each pack's status and disconnect them in case of any failure. The LVS and HVS are equipped with fuses, diodes, and relays which are responsible for managing various failures including overcurrent, overcharge, overheating, short circuit incidents, power drop, and connection loss with any board. Because of the capacitance load, the inverter is equipped with a pre-charging circuit.
Low Voltage Batteries	The LV system contains a secondary backup battery which is identical to the main one. It is switched to in the case that the main low voltage battery experiences a drop in voltage larger than 14V. It also has a voltage regulator to ensure the low voltage system always has a steady power supply.
Overheating Protection	The LIMs and all onboard PCBs have inbuilt overheating protection in the form of integrated temperature sensors and cooling system. The inverter utilises a customised cooling unit. Other components incorporate heat sinks, heat copper pipes, thermal paste, and heat pads. Also, the subsystem is mounted on an aluminium plate on top of the pod's structural frame, ensuring stability and ensures less exposure to heat form the LIM's.
Insulation	An insulation monitoring relay ensures proper insulation of the chassis and between windings and stator.
Braking Board	Any system failure results in the power to the brakes and motor being cut which engages the brakes and slows down the pod to a halt. The braking relays are handled by an 8-channel relay (Figure 4.1.4) board which is managed by the OBC through the CAN bus network.
Control	
Safety Structure	**Details**
Safety Flowchart for Control	Please see Figure 4.1.3 in the appendices, to see the safety flowchart showing how the system responds to various failure scenarios.
Communication	
Safety Structure	**Details**
Communication	If the inverter, brakes, or sensor board lose communication with the OBC because of loose wires, failure of OBC, or electromagnetic interruption, the brakes will automatically be engaged.

4. Appendices

4.1 Supporting Figures for the Electronics System

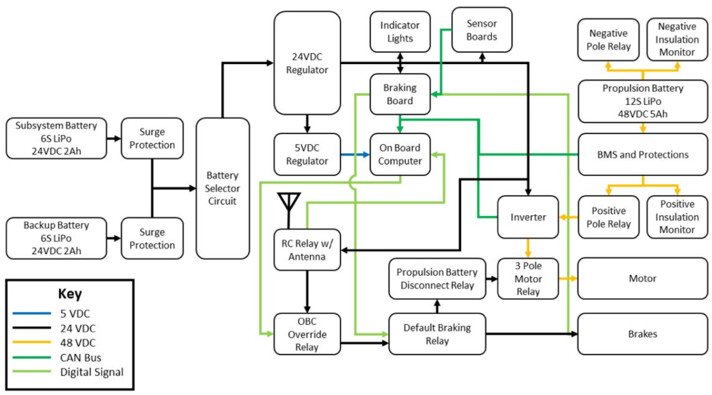

Figure 4.1.1: Low and High Voltage Power Circuitry of the Pod

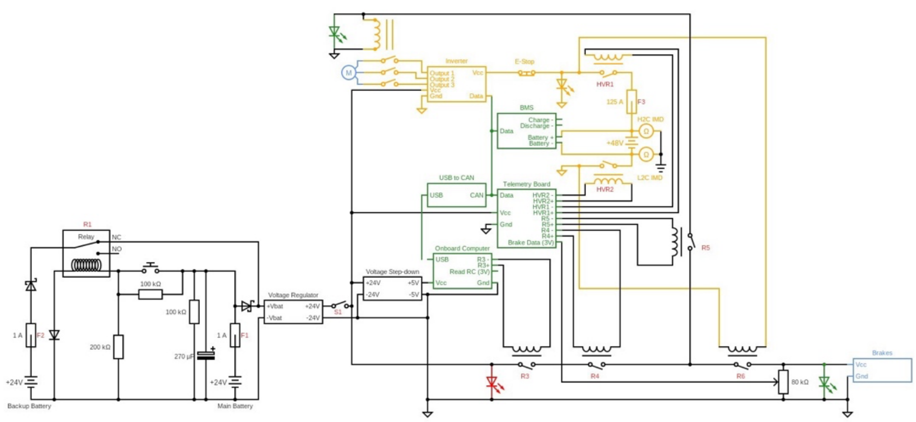

Figure 4.1.2: Circuit Diagram of the Electrical System

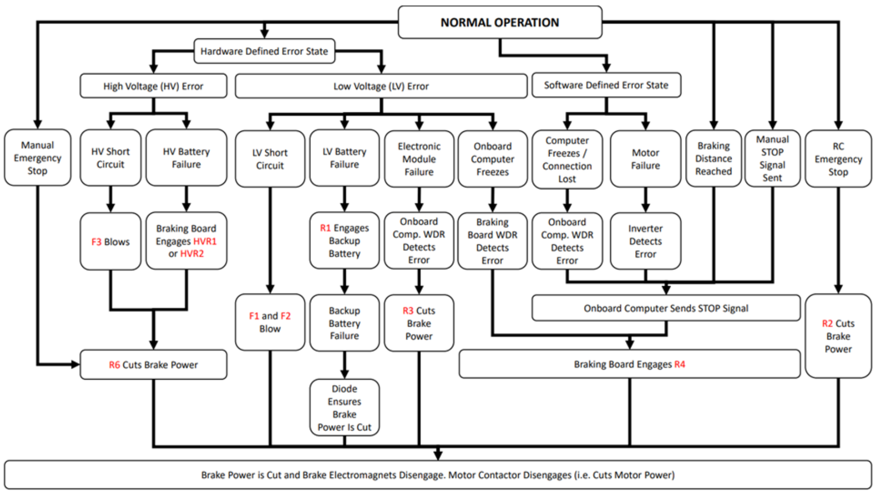

Figure 4.1.3: Failure Mitigation Flowchart

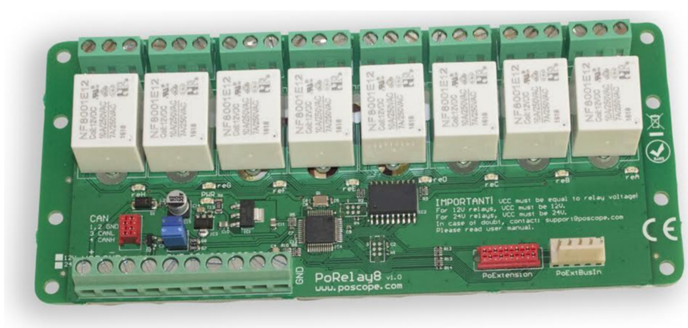

Figure 4.1.4: PoRelay8 – 8-Channel Relay Board

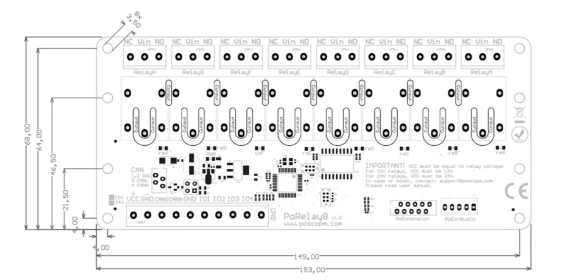

Figure 4.1.5: Mechanical Drawing and Dimensions of PoRelay8 Board

Figure 4.1.6: Bamobil D3 - Inverter

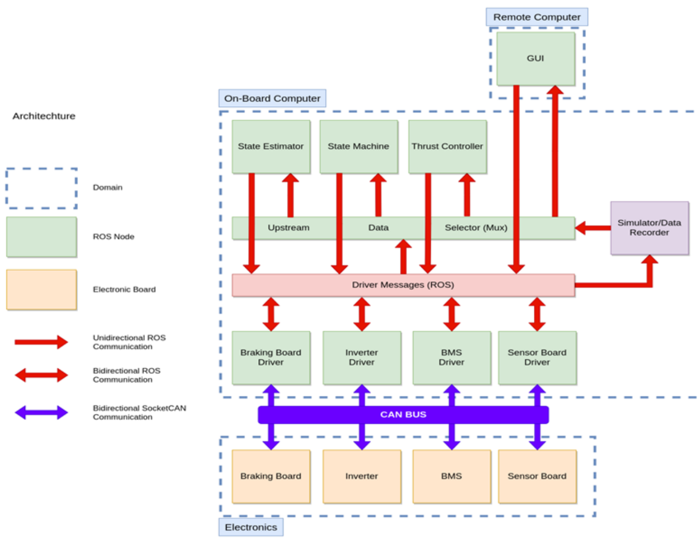

Figure 4.1.7 Software system architecture including the CAN bus networking layer, ROS backend, and GUI

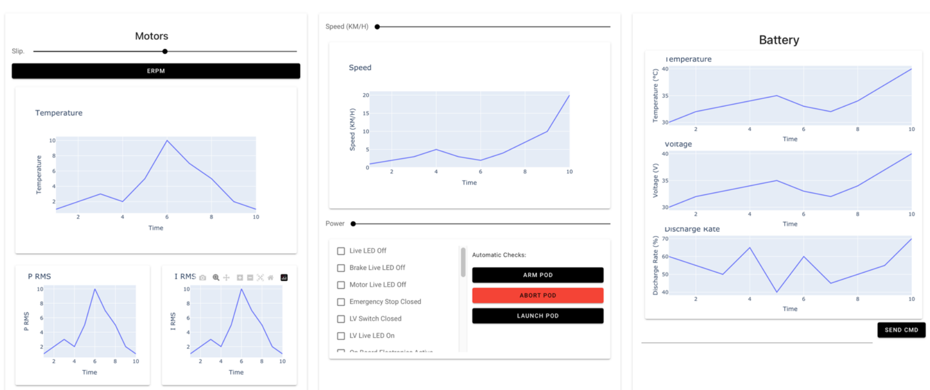

Figure 4.1.8 Current design for GUI which includes graphical representations for monitoring the state of the pod along with control options for automating transitions between the states of the system.

5. References

1. Chiba, A. (2005) ‘Stator Core’, in Magnetic bearings and bearingless drives. Amsterdam: Elsevier/Newnes.

2. Copper Development Association (no date) Copper is malleable & ductile, Official Site of Copper Development Association, Inc. (USA). Available at: https://www.copper.org/education/copper-is/elements/malleable-ductile.html (Accessed: 29 October 2024).

3. Electrical4U (2023) Understanding skin effect in transmission lines, Electrical4U. Available at: https://www.electrical4u.com/skin-effect-in-transmission-lines/ (Accessed: 29 October 2024).

4. Electrification, C. (2021) How thinner laminations improve power and performance in High Speed Motors, Carpenter Electrification.

5. Ion Boldea (2017). Linear Electric Machines, Drives, and MAGLEVs Handbook. CRC Press.

6. Laithwaite, E.R. (1970). Linear-motion Electrical Machines. IEEE Explore, pp.531–541.

7. Lesics (2021). Linear Motors | How do they work? [online] www.youtube.com. Available at: https://www.youtube.com/watch?v=uf_Z57gAJTc&t=302s [Accessed 29 October 2024].

8. Ningbo Jintian Copper (Group) Co., Ltd. (2023) Small size, big impact: The advantages of rectangular magnet wire in Electronics, Ningbo Jintian Copper (Group) Co., Ltd. Available at: https://jtcopper.com/the-advantages-of-rectangular-magnet-wire-in-electronics.html (Accessed: 28 October 2024).

9. Seydoux, M., Riva, N., Rametti, S., Benedetti, L., Dimier, T., Bollier, N. and Hodder, A. (2019). Design and manufacturing of a Linear Induction Motor for 2019 EPFLoop prototyle in the framework of the SpaceX Hyperloop competition. EPFL.

10. Shcherbakov, P. (2004) Magnetic properties of silicon electrical steels and its application in fast cycling superconducting magnets at low temperatures.

11. Skin effect (2023) Encyclopædia Britannica. Available at: https://www.britannica.com/science/skin-effect (Accessed: 28 October 2024).

12. The physics classroom tutorial (2023) The Physics Classroom. Available at: https://www.physicsclassroom.com/Class/thermalP/u18l1f.cfm (Accessed: 28 October 2024).

13. Timperio, C.L. (2018). Linear Induction Motors(LIM) for Hyperloop Pod Prototypes . Master Thesis.

14. WMD-sonja (2022) verope. Available at: https://verope.com/tech-videos/fill-factor-of-a-strand/#:~:text=The%20fill%20factor%20of%20a,smallest%20circle%20enclosing%20the%20strand. (Accessed: 29 October 2024).

15. Zickler, T.H. (2005) Basic design and engineering of normal-conducting, iron-dominated electromagnets.

16. Boldea, I. (2023) pg 16, in *Linear electric machines, drives, and maglevs Handbook*. Boca Raton: CRC Press (Accessed: 25 November 2023). [Accessed: 28 October 2024]

17. Research Gate. (2013) *(a) simulated B fi eld lines for a 47-magnet linear halbach array of* ... Available at: https://www.researchgate.net/figure/a-Simulated-B-fi-eld-lines-for-a-47-magnet-linear-Halbach-array-of-permanent-magnets_fig1_249992247 (Accessed: 28 October 2024).

18. Abdelrahman, A. S., J. Sayeed, and M. Z. Youssef. 2018. "Hyperloop Transportation System: Analysis, Design, Control, and Implementation." *IEEE Transactions on Industrial Electronics* 65 (9): 7427–7436.

19. Coty Nogah, 2023,The Advantages and Disadvantages of Neodymium Magnets: What You Need to Know,[online], Available at: https://www.dhgate.com/blog/the-advantages-and-disadvantages-of-neodymium-magnets-what-you-need-to-know-c/# [Accessed: 29 October 2024]